Finite-Amplitude Waves at the Interface between Fluids with Different Viscosity: Theory and Experiments

M. Sangalli, C. T. Gallagher, D. T. Leighton, H.-C. Chang, and M. J. McCready
Department of Chemical Engineering, University of Notre Dame, Notre Dame, Indiana 46556
(Received 23 September 1994; revised manuscript received 31 March 1995)

The interfacial instability caused by viscosity stratification of a density-matched two-layer, rotating Couette flow is examined close to criticality. Weakly nonlinear analysis of the full governing equations indicates that the instability is supercritical, and measurements of amplitudes for steady, traveling periodic waves agree well with the theoretical predictions.

PACS numbers: 47.20.Ma, 47.15.Fe, 47.20.Ky, 47.55.Hd

Flowing interfaces of stratified, immiscible fluids are common in our environment (e.g., wind-water) and in many kinds of industrial process equipment (e.g., condensers and oil transport pipelines). For this reason they have been the object of numerous studies both theoretically and experimentally [1]. Linear stability analyses predict that two-layer channel flows can be unstable to either long [2], moderate [3], or short [4] traveling waves. While the presence of six governing parameters prevents exhaustive studies, numerical techniques for the linearized problem have been developed to allow examination of all parameter and wave-number ranges [5–7]. Studies that examine weakly nonlinear evolution of the disturbances are relatively few in contrast. In the long-wave case it has been shown [8] that the evolution can be described by a Kuramoto-Sivashinsky equation, known to give rise to very rich dynamical behavior involving localized patterns. When the critical wave number is instead bounded away from zero, the classical bifurcation analysis yielding the Stuart-Landau or Ginzburg-Landau equation has been applied [9–11].

Experiments in gas-liquid systems show that interfacial waves can remain nearly periodic and small amplitude [12], evolve into roll waves [13], solitary waves [14], or slugs. However, it is difficult to find in the literature careful experiments that could be used to verify the quantitative predictions of both linear and nonlinear stability analyses. The presence of turbulence in the gas for gas-liquid systems prevents a direct application of rigorous analysis [12]. Even when the flow is laminar in both fluids, the common use of open flow systems poses additional difficulties. The usually convective nature of the instability results in "noise-sustained structures" [15] which evolve spatially [16]. The finite length of the apparatus in this case is a serious limit to the extent to which the evolution of the slowly growing disturbances close to neutral stability can be observed. The emerging patterns are not in general periodic in space, so that measurement of the amplitude in different locations is needed.

In this Letter we report on a novel experimental apparatus that reduces the uncertainty due to the above factors and allows direct comparison with theoretical predictions. This is achieved by a design that features the co-current flow of stratified fluids in a *closed* system. As a result, the wave patterns reach equilibrium amplitudes and can be observed in the system by waiting the appropriate amount of time. In addition, the flow is spatially periodic in nature, which allows a straightforward comparison with weakly nonlinear theory.

Two density-matched immiscible fluids are confined between concentric cylinders that are mounted on a Weissenberg rheogoniometer with the axis in the vertical direction (see Fig. 1). The diameters of inner and outer cylinders are 19.5 and 21.5 cm, respectively, with a resulting radial gap of 1 cm. The two Newtonian fluids used for the experiments reported here are Dow 710 (the outer fluid), which is a phenilmethyl polysiloxane, and a mixture of ethylene glycol, water, and Coffeemate—a commercial nondairy creamer that is used as a source of refractive particles. The viscosity and density of Dow 710 are 0.555 $\mathrm{N\,s/m^2}$ and 1110 $\mathrm{kg/m^3}$, respectively; the viscosity and density of the ethylene glycol solution are about 0.011 $\mathrm{N\,s/m^2}$ and 1108 $\mathrm{kg/m^3}$, respectively, while the surface tension between the two fluids is about 0.01 N/m. A *vertical* interface is formed by filling the device with the inner fluid and starting rotation. The Dow 710 is loaded on the rotating outer wall, and it displaces the glycol solution because it preferentially wets the outer cylinder. The process is aided by the slight

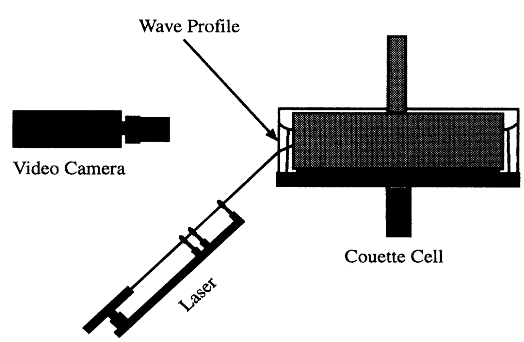

FIG. 1. The experimental apparatus and the horizontal laser setup.

density mismatch and by wiping the outer cylinder with 710 before it is loaded with the inner fluid. The bottom boundary is a layer of mercury that remains flat, and the top boundary is air. This limits the amount of shear in the vertical planes. As a result, when the outer cylinder is set in rotation with the inner cylinder kept fixed, a two-dimensional shear flow (in the horizontal plane) develops in the median section of the cell. This is the main advantage of our configuration over similar ones [17] where the interface is horizontal and in which the developed flow is likely to be fully three dimensional.

The position and shape of the interface are monitored by viewing through the transparent outer cylinder. Several lighting techniques are used for this purpose. Diffuse white light allows for a global picture of the flow field while vertical and horizontal He-Ne laser sheets are used for quantitative measurements of the interface position. In the vertical setup a plane of laser light is projected onto the interface at a large incidence angle. Laser light is visible at the surface of the outer cylinder and at the fluid-fluid interface. The distance between the two laser images is proportional to the fluid depth ratio. This image of the interface allows measurement of its vertical profile. The horizontal laser setup, shown in Fig. 1, is designed to detect the interface profile in the azimuthal direction at a fixed vertical position. The setup is calibrated by imaging a curved grid of known spacing. When the flow is stable, the interface is flat. When the instability sets in, this setup allows quantitative measurement of the waves developing in the azimuthal direction.

The ratio between the gap and the cylinder radii is about 1/10. This, together with the measured invariance of the interface in the vertical direction, allows modeling the system as a two-dimensional planar flow. The governing equations are the full Navier-Stokes equations in each phase coupled by continuity of velocity, normal and tangential stress balances, and the kinematic boundary condition at the unknown radial position of the interface. The standard domain perturbation technique is used to derive a weakly nonlinear version of the governing equation in terms of the deviation variables from the plane Couette base state. Nonlinearities up to cubic order are retained in the expansion. The resulting equations are equivalent to the ones used in Refs. [9,11]. A Chebyshev-tau spectral method is used to discretize the system of equations for numerical computations.

The eigenvalue problem governing the linear stability of the base state was solved numerically and with the long-wave analysis of [2] to determine onset conditions for the interfacial mode, the only one that can become unstable at low fluid velocities. When the physical characteristics of the fluids and the gap width are fixed, there are only two parameters that can be varied independently: the outer velocity U and the ratio of the fluid depths, quantified by the depth h of the less viscous fluid. The onset conditions in this parameter space for typical values of the

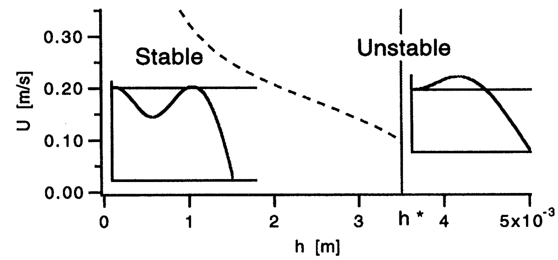

FIG. 2. Typical linear stability results for parameters corresponding to our experiment. The dashed line is the onset boundary for the short-wave instability. In the left inset the interfacial growth rate as the boundary is crossed is shown. In the right inset the interfacial growth rate in the long-wave instability region to the right of the solid line ($h = h^*$) is shown.

physical properties used in the experiments are shown in Fig. 2. When the less viscous fluid is sufficiently thin, the system is stable to long waves (a typical behavior for stratified flows) but can be unstable to short waves. In this region of short-wave instability there exists a critical value of rotation rate below which the Couette flow is stable and above which waves can be observed. A typical growth rate for the interfacial mode at criticality in this region is shown in the left inset. As the inner film thickness is increased, the critical wave number decreases, and reaches a vanishing value at a critical depth h^*. Beyond this point the instability is long wavelength in nature, and there is *no* critical rotation rate. The system is always unstable when the fluids are sheared, and the qualitative shape of the growth rate, shown in the right inset, is common to other long-wavelength instabilities such as the one exhibited by vertically falling films.

As the rotation speed is increased from the onset value, waves are predicted to grow in the system. The expected behavior is different for the short-wave case compared to the long-wave case. For the former, a small band of wave numbers bounded away from zero becomes unstable, and the disturbance wave number, at least close to criticality, is expected to be close to the critical one. In the second case, a band of wave numbers from zero to a cutoff value is unstable. The number of modes relevant to the nonlinear evolution is much larger in this case. In particular, the subharmonic instability is expected to appear in this system [18], and it is difficult to predict the selected wave number. A paradigm of this kind of system is the Kuramoto-Sivashinsky equation, in which chaotic dynamics involving localized solitary waves are observed.

The stability boundaries of the system are mapped experimentally by increasing the rotation rate of the outer cylinder until waves are detected. The observed behavior is consistent with the above theoretical results. In the short-wave region, periodic waves are first observed for conditions above the predicted onset with wave numbers belonging to the predicted range of unstable values. An example of the predicted neutral curve (solid line)

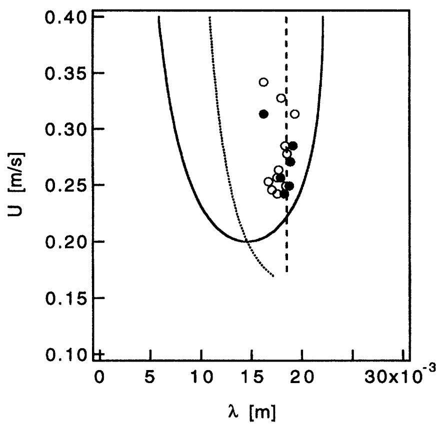

FIG. 3. The neutral curve predicted by linear stability (solid line) and the measured wavelengths for increasing plate speed. The inner film height and viscosity are 0.17 cm and 0.0115 $\mathrm{N\,s/m^2}$, respectively. The dotted line (maximum growing wave number) and the dashed line are the ones used in the computation of the amplitude values plotted with the same line type in Fig. 4.

compared to the observed wavelengths in this region is shown in Fig. 3. For depth ratios larger than the critical value, for which the predicted instability is of the long-wave variety, the observed periodic waves usually have wave numbers significantly lower than the maximum growing value. In some cases, the resulting waves have wavelength equal to the whole circumference and are very localized in nature.

The periodic nature of the waves observed in the region of short-wave instability warrants direct comparison with weakly nonlinear solutions obtained by bifurcation analysis of the governing equations. The deviation variables (velocity $\mathbf{u}$, pressure p, and interface position h) close to criticality are expanded in series of the eigenfunctions of the linear problem:

$$\phi = \begin{bmatrix} \mathbf{u} \\ p \\ h \end{bmatrix} = A\mathbf{v} + \overline{A\mathbf{v}} + \psi \,, \tag{1}$$

where $\mathbf{v}$ is the fundamental eigenfunction, ψ is a linear combination of the others, and the overbar denotes a complex conjugate. Center-unstable manifold theory allows leading order expression for the modes ψ which are stable at criticality as a function of the fundamental one. The result is the Stuart-Landau equation for the amplitude of the fundamental mode close to neutral stability

$$\dot{A} = \sigma A + \kappa |A|^2 A \,, \tag{2}$$

where κ is the Landau constant; its sign determines the nature of the instability. The computation of κ, although straightforward in principle, is rather involved due to the complexity of the governing equations and boundary conditions. The details are omitted here for brevity and the reader is referred to the papers by Renardy [10] and Blennerhassett [9] for similar formulations.

A couple of points deserve mention to illustrate the reasons why our setup is particularly appropriate for comparing nonlinear theory prediction and experiments. First, in the computation of two-dimensional finite-amplitude solution for parallel flows, an additional longitudinal boundary condition is needed to determine the solution. This is usually set to keep constant either the average flow rate or alternatively the average pressure drop. The difference between the formulations is evident even in plane Poiseuille flow [19]. In that case the resulting finite-amplitude solutions are found to be different depending on the chosen boundary condition, and to have different stability character [20]. In fact, a whole family of boundary conditions is possible, and therefore a family of solutions exists, as exploited by Barkley [21]. The same behavior is present for two-phase parallel flows and the corresponding analysis has revealed dramatic differences including the bifurcation switch from subcritical to supercritical [11], depending upon the selected condition. To compare with experiments, it is critical to know the correct boundary condition. Unfortunately, in an open flow system this can vary dramatically for different setups, and depend on the details of the sections of the apparatus preceding and following the one where the stratified flow is established. Most likely, the corresponding boundary condition will be somewhere between the two limiting cases and may not be easily determinable. In our experiment the closed and periodic nature of the flow dictates the absence of average pressure gradient in the azimuthal direction and therefore leaves no ambiguity as to the correct boundary condition. A further complication arises because of the presence of the interface between the two fluids. In addition to the critical eigenvalue at finite wave number, the interfacial mode is always neutrally stable for zero wave number. As a result, it is possible to excite an average shift of the interface, which will in turn modify the value of the Landau constant κ in Eq. (2) and consequently the equilibrium amplitude. This accounts for the difference between the finite-amplitude solutions studied in Ref. [11] and the ones studied in Ref. [9]. In an experiment carried out in an open flow system, the possibility of having a different average film height at different locations of the channel could make comparison with the theory difficult. The behavior in those systems has to be tackled by using coupled amplitude equations for the fundamental mode A and this second neutral mode B, as proposed in Ref. [11]. In the setup described in this Letter, the relative quantities of fluids are fixed and therefore the spatially averaged film height must remain constant. In other words, the amplitude B of the interfacial mode with zero wave number is always identically zero. In summary, in our system the Landau constant is uniquely determined by the fact that pressure gradient and average film height are fixed. When evaluated at criticality it is equivalent to the constant β in Ref. [11].

A code was written to compute the value of the constant κ. Its validity was checked by reproducing the numerical results reported for the Couette flow in [9,11]. In the region of short-wave instability, the code was used to test the nature of the bifurcation, which was found to be always supercritical. Furthermore, the dominant interaction that leads to saturation of the unstable mode is a *quadratic* interaction with the first overtone.

Comparison of measured and predicted wave amplitudes for a specific inner fluid depth ($h = 0.17$ cm) as the rotation rate is increased is shown in Fig. 4. The agreement is within experimental error and can be considered satisfactory. In particular, the predicted supercritical nature of the bifurcation was verified by measuring amplitudes for increasing (open circles in Fig. 4) and decreasing (full circles) the rotation rate. The absence of hysteresis expected in a supercritical bifurcation is evident in the data. Figure 5 shows an experimental wave profile detected with the horizontal laser setup compared to the corresponding one constructed as a finite-amplitude superposition of the fundamental eigenfunction, the mean flow, and the first harmonic. The amplitudes and relative phase differences of the above components are part of the information obtained by bifurcation analysis. Although only two harmonics are present in the reconstructed interfacial shape, their sum captures remarkably well the main features of the observed wave profile.

The success of these comparisons between theory and experiments for periodic wave patterns provides a basis for understanding more complex nonperiodic solutions that occur close to criticality in open flow experiments. In addition, the observed presence of localized interfacial structures when the instability is of the long-wave variety opens the possibility of a very careful study of these wave patterns common to many interfacial systems with similar growth rates. Again the advantage of having a closed system in which to observe the long-time evolution of these structures is extremely important.

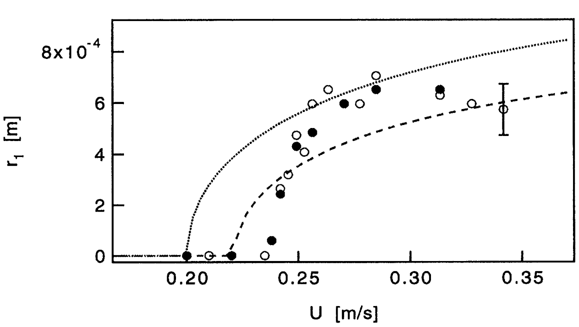

FIG. 4. The predicted and measured amplitudes for increasing (open circles) and decreasing (full circles) plate speed for the conditions shown in Fig. 3. The predicted curves are computed using as fundamental wave number the ones shown with the same line type in Fig. 3.

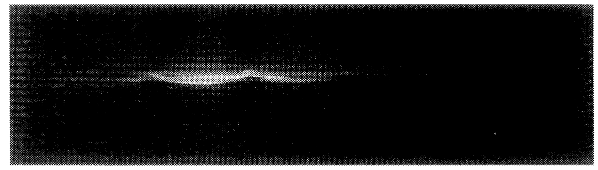

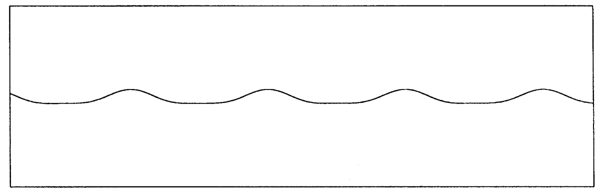

FIG. 5. The predicted (below) and measured interfacial shape. Viscosity and thickness of the inner fluid (above the interface in the figures) are 0.0115 N s/m^2 and 0.24 cm, respectively, while the outer plate speed is 29.5 cm/s.

This work has been supported by the NASA Microgravity Science and Applications Division under Grant No. NAG3-1398.

[1] D. D. Joseph and Y. Y. Renardy, *Fundamentals of Two-Fluid Dynamics* (Springer-Verlag, New York, 1992).
[2] C.-S. Yih, J. Fluid Mech. **27**, 337 (1967).
[3] L. S. Cohen and T. J. Hanratty, AIChE. J. **11**, 138 (1965).
[4] A. P. Hooper and W. G. C. Boyd, J. Fluid Mech. **128**, 507 (1983).
[5] S. G. Yiantsios and B. G. Higgins, Phys. Fluids **31**, 3225 (1988).
[6] A. P. Hooper, Phys. Fluids A **1**, 1133 (1989).
[7] Y. Renardy, Phys. Fluids **28**, 3441 (1985).
[8] A. P. Hooper and R. Grimshaw, Phys. Fluids **28**, 37 (1985).
[9] P. J. Blennerhassett, Philos. Trans. R. Soc. London A **298**, 451 (1980).
[10] Y. Renardy, Phys. Fluids A **1**, 1666 (1989).
[11] M. Renardy and Y. Renardy, Phys. Fluids A **5**, 2738 (1993).
[12] L. A. Jurman, S. E. Deutsch, and M. J. McCready, J. Fluid Mech. **238**, 187 (1992).
[13] T. J. Hanratty and A. Hershman, AIChE. J. **7**, 488 (1961).
[14] L. A. Jurman and M. J. McCready, Phys. Fluids A **1**, 522 (1989).
[15] R. Deissler, J. Stat. Phys. **54**, 1459 (1989).
[16] M. Sangalli *et al.,* Chem. Eng. Sci. **47**, 3289 (1992).
[17] F. Charru and J. Fabre, in *Instabilities in Multiphase Flows,* edited by G. Gousbet and A. Berlemont (Plenum Press, New York, 1993), p. 205.
[18] M. Cheng and H.-C. Chang, Phys. Fluids A **4**, 505 (1992).
[19] J. D. Pugh and P. G. Saffman, J. Fluid Mech. **194**, 295 (1988).
[20] I. Soibelman and D. I. Meiron, J. Fluid Mech. **229**, 389 (1991).
[21] D. Barkley, Phys. Fluids A **2**, 955 (1990).

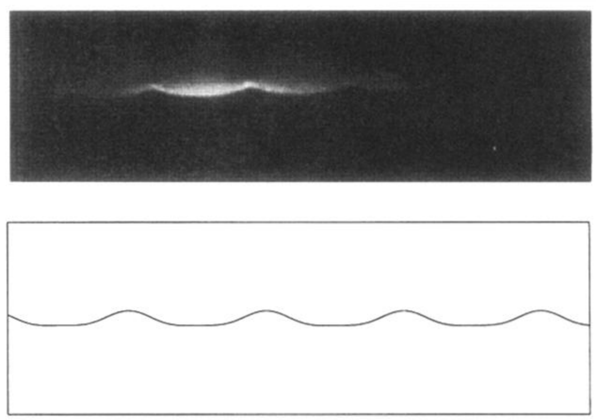

FIG. 5. The predicted (below) and measured interfacial shape. Viscosity and thickness of the inner fluid (above the interface in the figures) are 0.0115 $\mathrm{N\,s/m^2}$ and 0.24 cm, respectively, while the outer plate speed is 29.5 cm/s.